Polarization imaging in atmospheric environment based on polarized reflectance retrieval

Huijie Zhao (赵慧洁)[1,*], Jian Xing (邢 健)[1], Xingfa Gu (顾行发)[2], and Guorui Jia (贾国瑞)[1,]**

[1]*School of Instrumentation Science and Opto-electronics Engineering, Beihang University, Beijing 100191, China*
[2]*Institute of Remote Sensing and Digital Earth, Chinese Academy of Sciences, Beijing 100094, China*
**Corresponding author: hjzhao@buaa.edu.cn; **corresponding author: jiaguorui@buaa.edu.cn*
Received July 7, 2018; accepted November 12, 2018; posted online December 20, 2018

A method for calculating the atmospheric parameters measurement accuracy requirement based on polarized reflectance retrieval is proposed. The at-sensor polarization states with different atmospheric parameters content are simulated based on the atmospheric radiative transfer model in order to select the key parameter affecting the polarization observation. The accuracy requirement of atmospheric parameters is derived through the polarized reflectance retrieval method. Experiment results show that retrieval accuracy of polarized reflectance of typical ground objects can be up to 90%. The atmospheric parameters measurement accuracy requirement when the retrieval accuracy is more than 75% is derived.

OCIS codes: 260.5430, 110.5405, 290.1483.
doi: 10.3788/COL201917.012601.

The polarization characteristic of ground objects is an important component of the earth remote sensing database. Most of the existing polarization detection research is based on polarization degree (DOP) and polarization angle (AOP) of at-sensor radiance, which can enhance objects of interest or restrain background disturbance qualitatively[1–8]. However, polarized reflectance of ground objects was not involved in the above studies. Polarized images obtained by the sensor contain polarized contributions on the atmospheric radiation transmission path, but the polarization characteristics of the object could not be quantitatively retrieved. This will produce different results under different observation conditions[9], creating greater instability. To quantify remote sensing for ground polarization, it is necessary to calculate the polarized reflectance of ground objects accurately. The polarized reflectance of a ground object is the polarized reflection part in its overall reflectance, which is the ratio of polarized components of the reflected radiance against the incident radiance[10]. Referring to the retrieval method of ground surface reflectance based on the scalar atmospheric radiative transfer model[11], a lookup table (LUT) with surface reflectance, observation conditions, and at-sensor polarization states is established based on the second simulation of a satellite signal in the solar spectrum–vector (6SV) model[12] and surface polarized reflectance is retrieved by polarized images through the LUT and numerical calculation.

The measurement of atmospheric parameters is very important for the ground polarization observation. Since the atmosphere is constantly changing during the course of the experiment, the data will be distorted if the atmosphere effect is ignored. However, atmospheric parameters are usually unable to have full-time coverage measurements due to some practical factors. So, the measurement accuracy requirement of atmospheric parameters needs to be ensured for a more rational experiment approach. A method for calculating measurement accuracy requirements of atmospheric parameters based on polarized reflectance retrieval was proposed. The key parameter in ground polarization observation is determined by simulating the atmospheric radiative transfer model. An atmospheric parameter range with reasonable retrieval accuracy is obtained through the polarized reflectance retrieval method, which can be applied to different observation conditions. The efficiency of filtering effective data in measurement can be significantly improved.

The at-sensor polarization states with different atmospheric parameters content are simulated based on the atmospheric radiative transfer model. Polarized reflectance is obtained through the retrieval method, and the atmospheric parameter range with reasonable retrieval accuracy is derived by adjusting the key parameter content in the retrieval calculation. Thus, the accuracy requirement of atmospheric parameters is derived.

Water vapor, ozone, and aerosol are selected to simulate the polarized radiative transfer process by the control variate method. Results are shown in Fig. 1.

The at-sensor DOP is the ratio of the apparent polarized radiance against the apparent radiance. The scattering of water molecules is Rayleigh scattering, while atmospheric polarization properties are usually influenced by large size molecules, i.e., Mie scattering. However, water vapor content has a significant influence on atmospheric transmittance in the water vapor absorption band to thus influence apparent radiance and apparent polarized radiance, which could not be ignored. In the water vapor non-absorption band, the vapor content has almost no effect on the atmospheric transmittance, so the apparent radiance and the apparent polarized

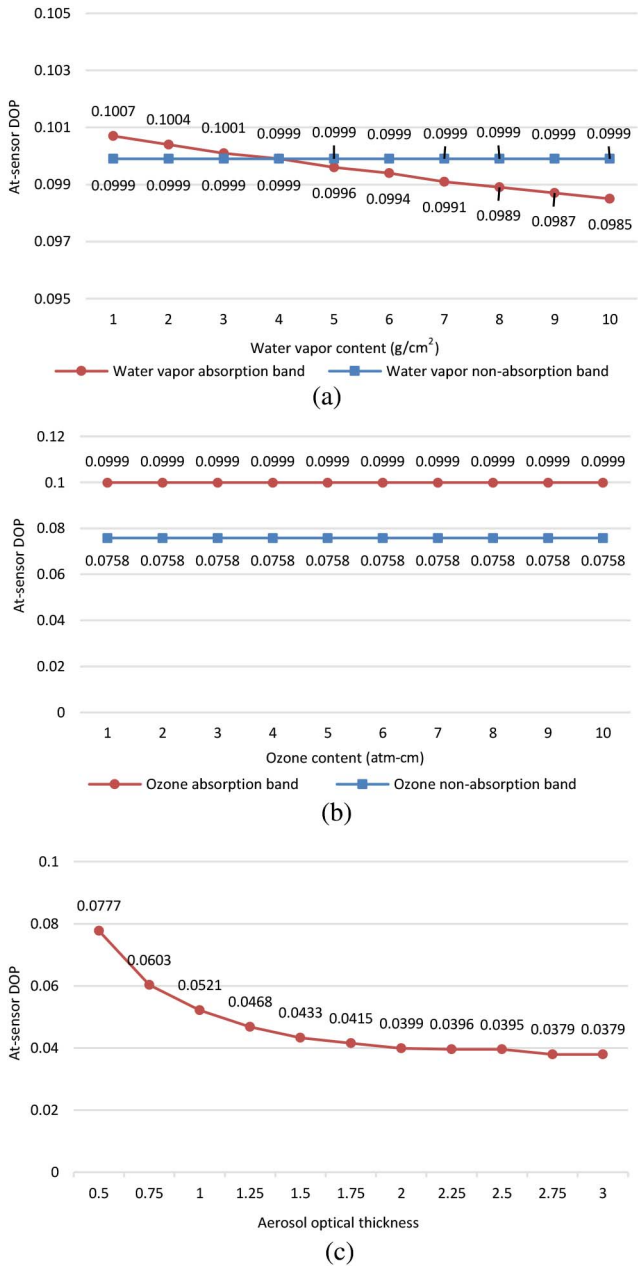

Fig. 1. Influence of atmosphere parameters (solar zenith angle = 25°, view zenith angle = 45°, relative azimuth angle = 60°, elevation = 1 km, reflectance = 0.25). (a) Influence of water vapor (ozone content = 3 atm-cm, visibility > 5 km), (b) influence of ozone (water vapor content = 2.0 g/cm^2, visibility > 5 km), (c) influence of aerosol optical thickness (ozone content = 3 atm-cm, water vapor content = 2.0 g/cm^2).

radiance will not be affected either. Similarly, it is found that the ozone content has very little effect on at-sensor DOP.

The aerosol optical thickness (AOT) has significant effects on at-sensor DOP. With the increase of AOT, at-sensor DOP decreases gradually. But, the influence is attenuated when the AOT is less than a certain value due to the decreasing of visibility. The AOT strongly affects the polarization observation of the ground objects. Also, the absorption band of water vapor should be avoided, so as to reduce the interference of the water vapor contribution to the polarization characteristics of the ground objects as much as possible.

The retrieval process of ground object polarized reflectance is as follows: deriving at-sensor polarization states (DOP & AOP) of reflected radiation by polarized images; finding at-sensor polarization states in the LUT; ensuring polarized reflectance through interpolation.

The at-sensor radiance $\overrightarrow{L}_s$ is composed of three parts: (1) direct solar reflection from the target ($\overrightarrow{L}_r$), randomly polarized incident flux bidirectionally reflected and polarized by the target and propagated to the sensor; (2) target-reflected downwelled radiance from the skydome ($\overrightarrow{L}_d$), randomly polarized solar illumination scattered and polarized by the atmosphere and propagated to the target, where it is polarimetrically bidirectionally reflected and integrated over the hemisphere above the target; (3) upwelled atmospheric radiance resulting from solar scatter along the target to the sensor path ($\overrightarrow{L}_u$), randomly polarized solar illumination scattered and polarized by the atmosphere and propagated to the sensor[13],

$$\overrightarrow{L}_s = \overrightarrow{L}_r + \overrightarrow{L}_d + \overrightarrow{L}_u, \tag{1}$$

where

$$\overrightarrow{L}_r = T_r(\theta_r)\boldsymbol{F}_r(\theta_i,\theta_r,\varphi)\,T_i(\theta_i)\cos\theta_i E_s(\theta_i), \tag{2}$$

$$\overrightarrow{L}_d = T_r(\theta_r)\iint_{\Omega_i}\boldsymbol{F}_r(\theta_i,\theta_r,\varphi)\cos\theta_i\,\overrightarrow{L}_d^{\Omega_i}(\theta_i,\varphi_i)\,\mathrm{d}\Omega_i, \tag{3}$$

$$\overrightarrow{L}_u = \overrightarrow{L}_u(\theta_r,\varphi_r), \tag{4}$$

where E_s is exoatmospheric solar irradiance, T_i is transmittance of the solar-to-target path, T_r is transmittance of ground-to-sensor path, θ_i is the incident zenith angle, θ_r is the reflected zenith angle, φ is the relative azimuth angle, φ_i is the incident azimuth angle, φ_r is the reflected azimuth angle, $\boldsymbol{F}_r$ is the polarized bidirectional reflectance distribution function (pBRDF)[14], $\overrightarrow{L}_d^{\Omega_i}$ is the downwelled radiance distributed over the entire sky hemisphere, and $\mathrm{d}\Omega_i = \sin\theta_i\mathrm{d}\theta_i\mathrm{d}\varphi$ [sr].

Substituting Eqs. (2)–(4),

$$T_r\boldsymbol{F}_r T_i\cos\theta_i E_s = \overrightarrow{L}_s - T_r\iint_{\Omega_i}\boldsymbol{F}_r\cos\theta_i\,\overrightarrow{L}_d^{\Omega_i}\mathrm{d}\Omega_i - \overrightarrow{L}_u. \tag{5}$$

Since exoatmospheric irradiance is randomly polarized, we can only take consideration of the first column of the pBRDF Mueller matrix (representing the energy exchange at the optical element and relating the Stokes vector of the incident and exiting beams)[15] in the $\overrightarrow{L}_r$ expression when the specular component of reflected flux is dominated by direct solar reflection. Equation (5) may be expressed as

$$T_r\begin{bmatrix} f_{00} \\ f_{10} \\ f_{20} \end{bmatrix} T_i \cos\theta_i E_s = \overrightarrow{L}_s - T_r \iint_{\Omega_i} \boldsymbol{F}_r \cos\theta_i \overrightarrow{L}_d^{\Omega_i} \mathrm{d}\boldsymbol{\Omega}_i - \overrightarrow{L}_u, \tag{6}$$

$$\begin{bmatrix} f_{00} \\ f_{10} \\ f_{20} \end{bmatrix} = \frac{\overrightarrow{L}_s - T_r \iint_{\Omega_i} \boldsymbol{F}_r \cos\theta_i \overrightarrow{L}_d^{\Omega_i} \mathrm{d}\boldsymbol{\Omega}_i - \overrightarrow{L}_u}{T_r T_i \cos\theta_i E_s}. \tag{7}$$

In visible and near infrared bands, $\overrightarrow{L}_r$ is 5–10 times that of $\overrightarrow{L}_d$[13]. So, we consider $\overrightarrow{L}_d$ as an "error term", and then Eq. (7) can be rewritten as

$$\begin{aligned} \begin{bmatrix} f_{00} \\ f_{10} \\ f_{20} \end{bmatrix} &= \frac{\overrightarrow{L}_s - \overrightarrow{L}_u}{T_r T_i \cos\theta_i E_s} - \frac{T_r \iint_{\Omega_i} \boldsymbol{F}_r \cos\theta_i \overrightarrow{L}_d^{\Omega_i} \mathrm{d}\boldsymbol{\Omega}_i}{T_r T_i \cos\theta_i E_s} \\ &= \frac{\overrightarrow{L}_s - \overrightarrow{L}_u}{T_r T_i \cos\theta_i E_s} - \begin{bmatrix} \varepsilon_0 \\ \varepsilon_1 \\ \varepsilon_2 \end{bmatrix}, \end{aligned} \tag{8}$$

$$\begin{bmatrix} f_{00}+\varepsilon_0 \\ f_{10}+\varepsilon_1 \\ f_{20}+\varepsilon_2 \end{bmatrix} = \frac{\overrightarrow{L}_s - \overrightarrow{L}_u}{T_r T_i \cos\theta_i E_s}. \tag{9}$$

This "error term" is determined by sky light and the polarized reflectance of the ground object, which is difficult to solve directly, so we need to set up the LUT of at-sensor polarization states and observation conditions (geometric parameters, atmospheric parameters, polarized reflectance of objects). The formula mentioned above is hard to derive the analytic solutions of pBRDF. With the approach shown in Fig. 2, pBRDF can be retrieved by remote sensing images, and then the polarized reflectance of objects could be obtained through the pBRDF numerical solutions.

The Stokes vectors of at-sensor radiance are obtained by image processing, then DOP and AOP are expressed as

$$\begin{aligned} \alpha &= \frac{\sqrt{Q^2+U^2}}{I}, \\ \eta &= \frac{1}{2}\arctan\frac{U}{Q}, \end{aligned} \tag{10}$$

where α is the DOP of the at-sensor radiance, η is the AOP of the at-sensor radiance, and $[I, Q, U]$ are the Stokes vectors of the at-sensor radiance. At the same time, auxiliary information of polarization images (including atmosphere types, aerosol types, and wavelength) is obtained; geometric conditions (incident zenith angle, reflected zenith angle, and relative azimuth angle) are obtained by other instruments. The above data is put into the LUT, and then polarized reflectance of the object under one observation condition is obtained by retrieval and matching.

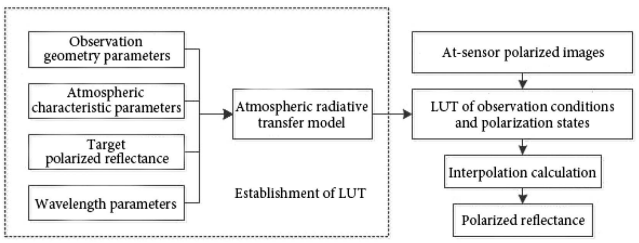

Fig. 2. Flow chart of polarized reflectance retrieval.

In Eq. (9), $\overrightarrow{L}_s$ is obtained from the sensor, E_s, θ_i, and $\overrightarrow{L}_u$ are determined by observation geometry in the LUT, and T_i and T_r are determined by aerosol type in the LUT. The input of LUT consists of geometric conditions, atmospheric types, aerosol types, wavelength, elevation, different reflectance, and polarized reflectance, and the output is the simulation value of at-sensor DOP and AOP. Repeat this process several times to create the LUT. Thresholding and the linear interpolation method are used in order to determine the polarized reflectance of each pixel in the polarization images.

Polarized reflectance is obtained through the retrieval method, and the atmospheric parameter range with reasonable retrieval accuracy is derived by adjusting the content of the key parameters in the retrieval process. The steps are as follows.

(1) For laboratory observation data under certain conditions, 6SV is used to generate the at-sensor DOP simulation data with the setting of AOT and elevation.
(2) LUT of polarized reflectance and at-sensor DOP is obtained by changing the AOT. Polarized reflectance is derived with the at-sensor DOP simulation data in step (1).
(3) The standard and retrieval value of each pixel in step (2) is compared by root mean square error (RMSE). The detection error of AOT is acceptable when the RMSE is less than a setting threshold. Step (2) is repeated until the measurement accuracy range of the atmospheric parameter is obtained.

Experiments are developed for verifying the proposed retrieval method. The objects are observed in the laboratory and outdoors, respectively, and the standard and retrieval values of polarized reflectance are obtained. The precision of the retrieval method is verified by comparisons.

As shown in Fig. 3, polarization images are obtained by a polarized imager based on the liquid crystal variable retarder (LCVR)[15]. Halogen lamps are used as a light source (they can be considered as natural light). As the distance between the light source and the object is short enough, atmosphere effects can be ignored. DOP and AOP of at-sensor radiance are derived from experiment data, and polarized reflectance is retrieved as the standard value[15].

Images of a painted metal board on land are obtained by the sensor located atop a high building. The polarized images of outdoor experiments at 676 nm are shown in Fig. 4. AOT and water vapor data are measured synchronously. AOT = 0.149 at 676 nm, and water vapor content equals 1.67 g/cm^2. Then, DOP and AOP of at-sensor radiance

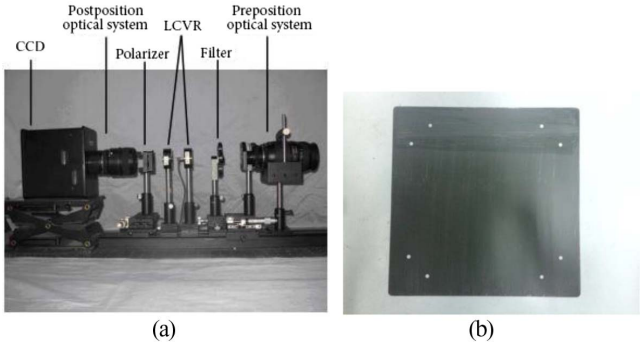

Fig. 3. LCVR imager and laboratory experiment. (a) LCVR imager and (b) painted metal board.

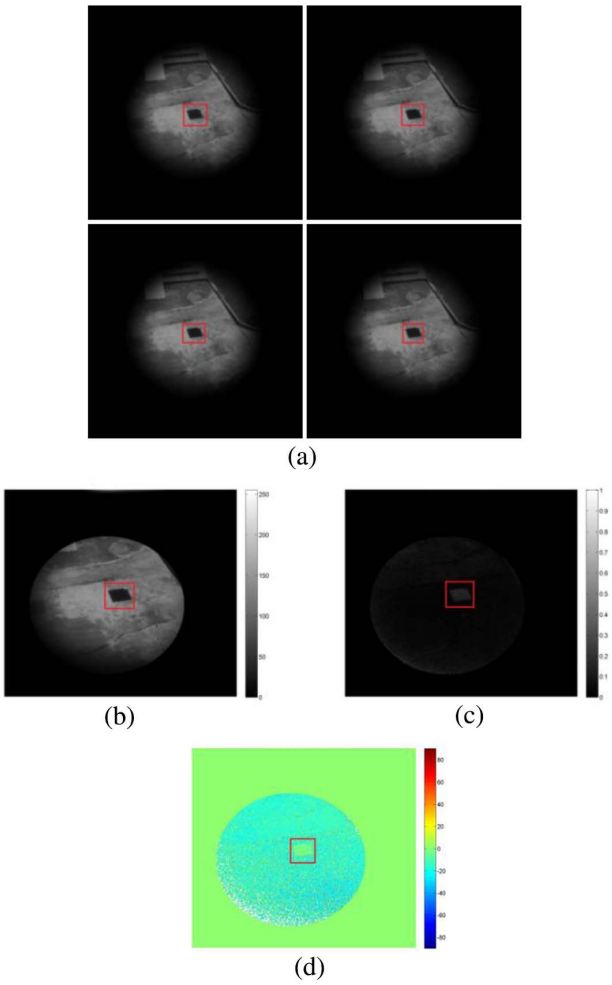

Fig. 4. Polarization images and processed images of painted metal board obtained from outdoor experiments (wavelength = 676 nm, solar zenith angle = 25°, view zenith angle = 45°, relative azimuth angle = 60°). (a) Original polarization images, (b) intensity image, (c) polarization degree image, (d) polarization angle image.

are derived from experiment data for polarized reflectance retrieval[15].

The target polarization characteristics retrieval is carried out pixel by pixel, and each pixel corresponds to a polarized reflectance r_p. For a single pixel, the error can be expressed as

$$e_{ij} = \frac{|r_{ij} - r_{ij}^0|}{r_{ij}^0} \times 100\%, \tag{11}$$

where i and j are integers, representing the number of sample pixels in the polarized images, r_{ij} is the calculation value of polarized reflectance, and r_{ij}^0 is the standard value of polarized reflectance. The polarized reflectance relative error of the whole polarized image can be expressed as

$$M_r = \sqrt{\frac{\sum_n e_{ij}^2}{n}} \times 100\%, \tag{12}$$

which represents the accuracy of the retrieval method.

According to the above precision evaluation method, results are shown in Fig. 5, and the retrieval error is 9.6%.

The calculation method of the atmospheric parameters measurement accuracy requirement is illustrated by experiment data obtained above. The observation condition is set as follows: AOT = 0.3 (average value of clear sky), elevation = 1 km, solar zenith angle = 25°, view zenith angle = 45°, relative azimuth angle = 60°, wavelength = 676 nm, the RMSE threshold is set to 25% for an acceptable retrieval accuracy, the AOT detection accuracy range is ensured by enumeration, and the result is $(0, 0.5)$ and shown in Fig. 6.

There are some probable reasons for the error.

(1) The projecting angle of the halogen lamp is about 5°, so it is sometimes difficult to ensure identical geometric angles in the same image.
(2) The calibration accuracy of the LCVR used in the experiment is higher than 95%[15], causing some errors in image processing and calculation.
(3) The retrieval algorithm is based on the atmospheric radiative transfer model. Errors may also be brought into account in the process of LUT establishment, thus affecting the results of retrieval.

The LUT of observation conditions and at-sensor polarization states has been proposed for the polarized reflection characteristics detection of ground targets. Polarized reflectance of targets has been retrieved with accuracy analysis. On this basis, the calculation method of the atmospheric parameters measurement accuracy requirement and its operation example have been proposed through the atmospheric parameter analysis.

Polarization observation experiments of painted metal targets are developed on a ground surface. Compared with laboratory experiments, the accuracy of polarized reflectance retrieval has been verified: the retrieval error is 9.6% at the wavelength of 676 nm, which means that the retrieval accuracy is better than 90%. When the retrieval error requirement is less than 25% under AOT = 0.3 condition, the AOT detection accuracy range is $(0, 0.5)$.

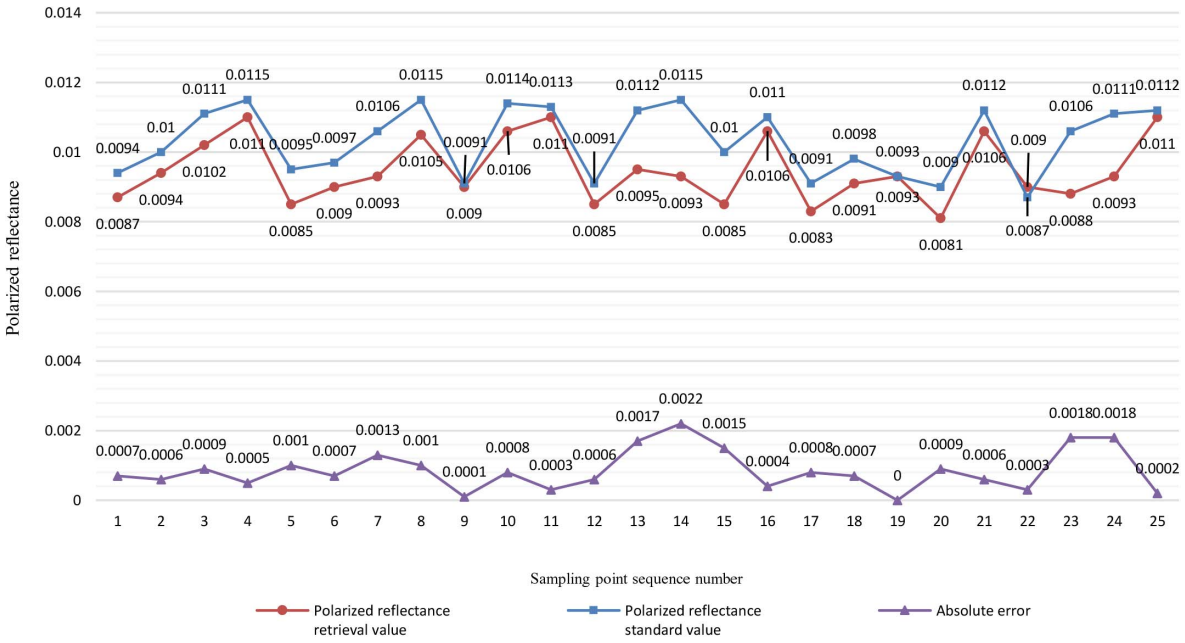

Fig. 5. Experiment results of painted metal board at 676 nm.

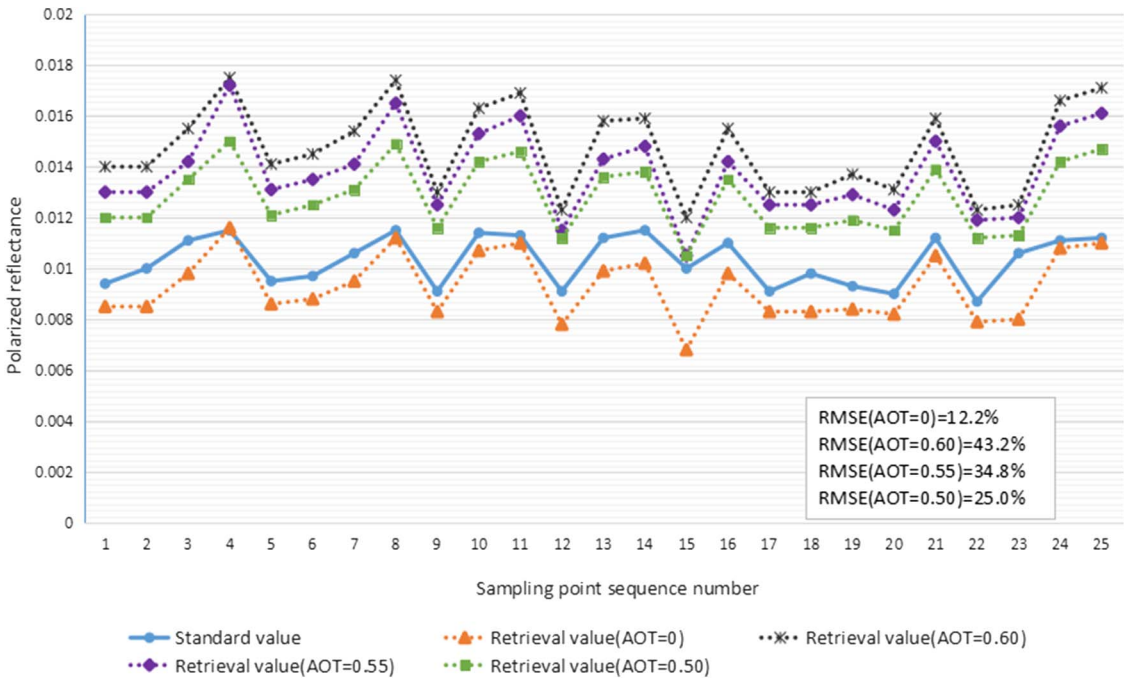

Fig. 6. Retrieval results in the AOT condition of 0, 0.30, 0.50, 0.55, and 0.60.

Compared with existing retrieval methods, adaptability to various observation conditions is improved. On this basis, a calculation method of the atmospheric parameters measurement accuracy requirement has been proposed through the atmospheric parameter analysis, which can adapt to many observation conditions and can be used for improving the polarization observation scheme. At-sensor polarization data under different atmospheric parameters are obtained in the process of research to accumulate data for a digital earth database. In addition, the directions of theoretical research and experimental schemes for further improvement have been suggested through the error analysis: using the pixel fusion method to solve the geometric inconsistency caused by the light projection angle, improving the measurement accuracy and the calibration accuracy of the sensor for further use, and improving the effective number digits of simulated data based on existing models to reduce rounding errors.

This work was supported by the National Natural Science Foundation of China (NSFC) (No. 61675012) and the National Key Research and Development Program of China (NKRDPC) (No. 2016YFB0500502).

References

1. D. Goldstein, Proc. SPIE **4133**, 112 (2000).
2. G. Forssell and K. E. Hedbory, Proc. SPIE **5075**, 246 (2003).
3. S. Q. Yang, "Ground-air separation verification based on polarization neutral points," Master Dissertation (Capital Normal University, 2014).
4. C. Y. Zhang, H. F. Cheng, and Z. H. Chen, J. Infrared Millim. W. **28**, 137 (2009).
5. Q. C. Wang, D. P. Zhao, and J. C. Wang, Opto-electronic Eng. **40**, 29 (2013).
6. Y. Han, W. R. Xu, and L. Jin, J. Infrared Millim. W. **34**, 606 (2015).
7. P. Xia and X. B. Liu, Spectrosc. Spect. Anal. **37**, 2331 (2017).
8. J. Zhu, X. H. Wang, and B. L. Pan, Spectrosc. Spect. Anal. **32**, 1913 (2012).
9. L. Yan, W. Chen, Y. Xiang, B. Yang, and Y. S. Zhao, *Physics of Polarization Remote Sensing* (Science, 2014).
10. F. M. Breon, D. Tanre, and P. Lecomte, IEEE. Trans. Geosci. Remote **33**, 487 (1995).
11. G. R. Jia, A. Hueni, and D. X. Tao, Opt. Express. **24**, 19905 (2016).
12. E. D. Vermote, D. Tanré, and J. L. Deuzé, "Second simulation of a satellite signal in the solar spectrum–vector," http://6s.ltdri.org (November 6, 2006).
13. J. R. Schott, *Fundamentals of Polarimetric Remote Sensing* (SPIE, 2009).
14. J. R. Shell, "Polarimetric remote sensing in the visible to near infrared," PhD Dissertation (Rochester Institute of Technology, 2005).
15. H. B. Zhao, "Research on polarization detection technique based on LCVR," Master Dissertation (Beihang University, 2008).